Electronic Supplementary Information

Long-lived fluorinated boron-nitride dots exhibiting room-temperature phosphorescence and high-temperature resistance

Xu Zhang,[a] Shenghui Han,[a] Gang Lian,*[a] Deliang Cui[a] and Qilong Wang[b]

a. State Key Lab of Crystal Materials, Shandong University, Jinan 250100, P.R. China.

b. Key Laboratory for Special Functional Aggregated Materials of Education Ministry, School of Chemistry & Chemical Engineering, Shandong University, Jinan 250100, P.R. China.

email: liangang@sdu.edu.cn

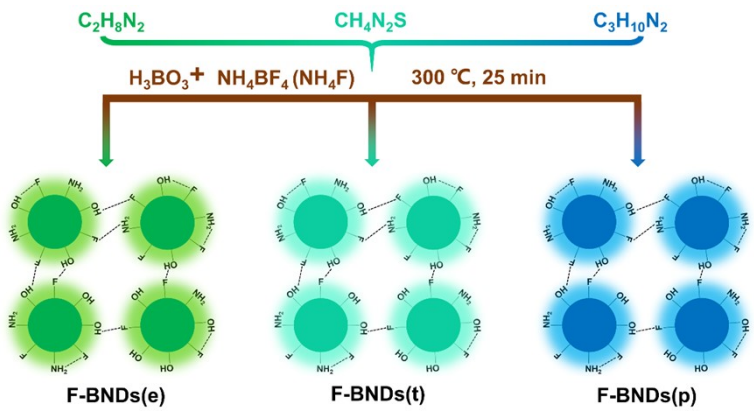

Fig. S1 Synthetic procedures of F-BNDs(e), F-BNDs(t) and F-BNDs(p).

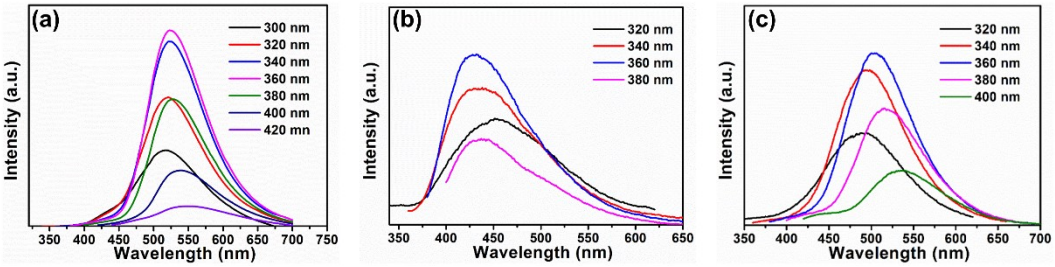

Fig. S2 The phosphorescence emission spectra excited at different wavelengths of (a) F-BNDs(e), (b) F-BNDs(p) and (c) F-BNDs(t).

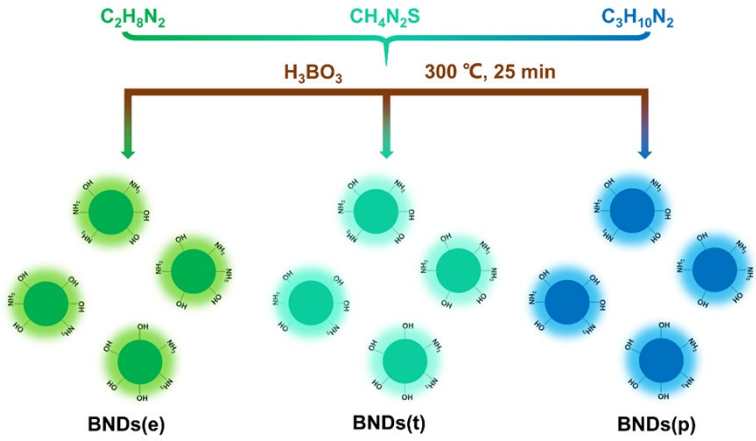

Fig. S3 Synthetic procedures of BNDs(e), BNDs(t) and BNDs(p).

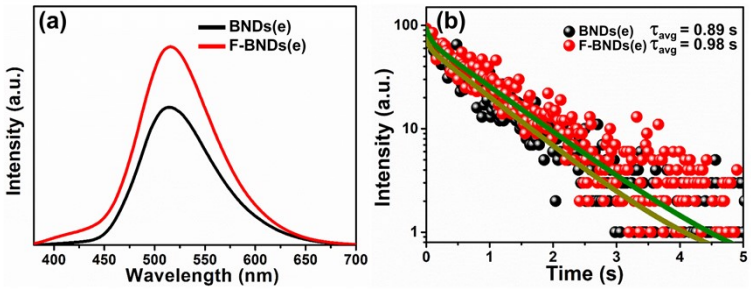

Fig. S4 (a) The phosphorescence emission spectra of F-BNDs(e) and BNDs(e) under 360 nm excitation. (b)Time-resolved phosphorescence decay curves of F-BNDs(e) and BNDs(e) under 360 nm excitation.

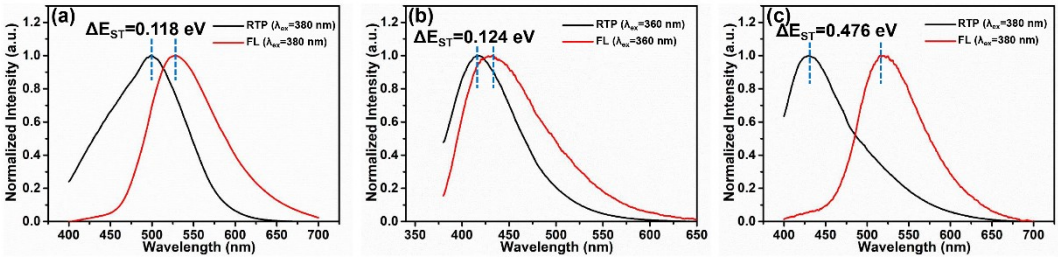

Fig. S5 FL and phosphorescence spectra excited at 360 nm of (a) F-BNDs(e), (b) F-BNDs(p) and (c) F-BNDs(t).

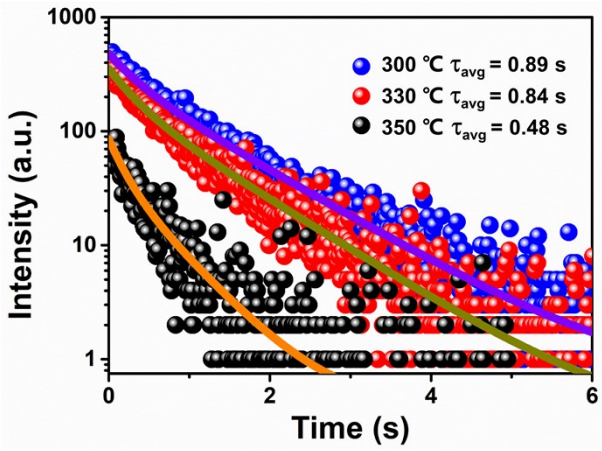

Fig. S6 Time-resolved phosphorescence decay curves of BNDs(e) obtained at 300, 330 and 350 ℃.

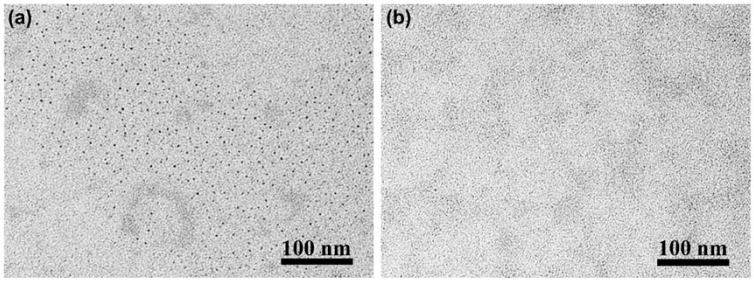

Fig. S7 TEM images of (a) F-BNDs(p) and (b) F-BNDs(t).

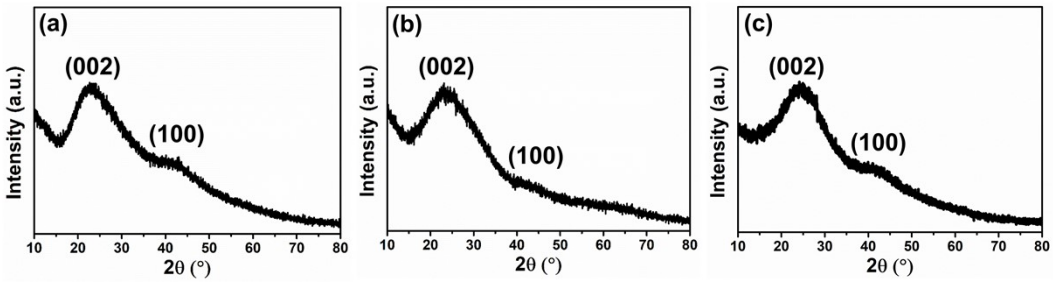

Fig. S8 XRD patterns of (a) F-BNDs(e), (b) F-BNDs(p) and (c) F-BNDs(t).

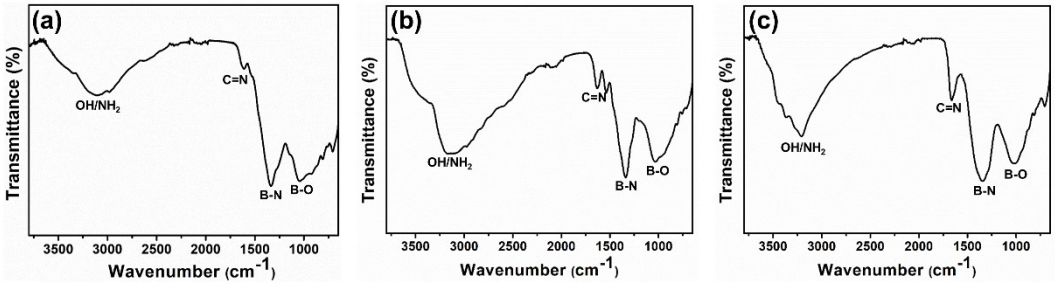

Fig. S9 FTIR spectra of (a) F-BNDs(e), (b) F-BNDs(p) and (c) F-BNDs(t).

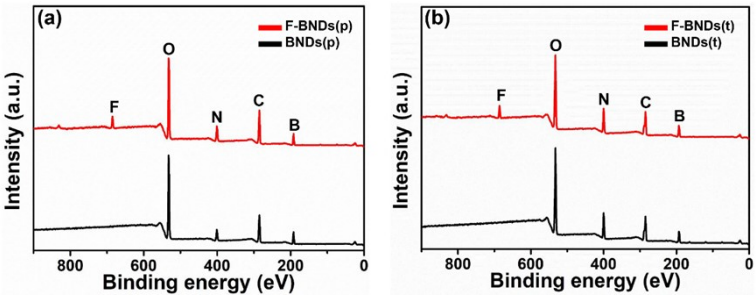

Fig. S10 (a) The survey XPS spectra of F-BNDs(p) and BNDs(p). (b) The survey XPS spectra of F-BNDs(t) and BNDs(t).

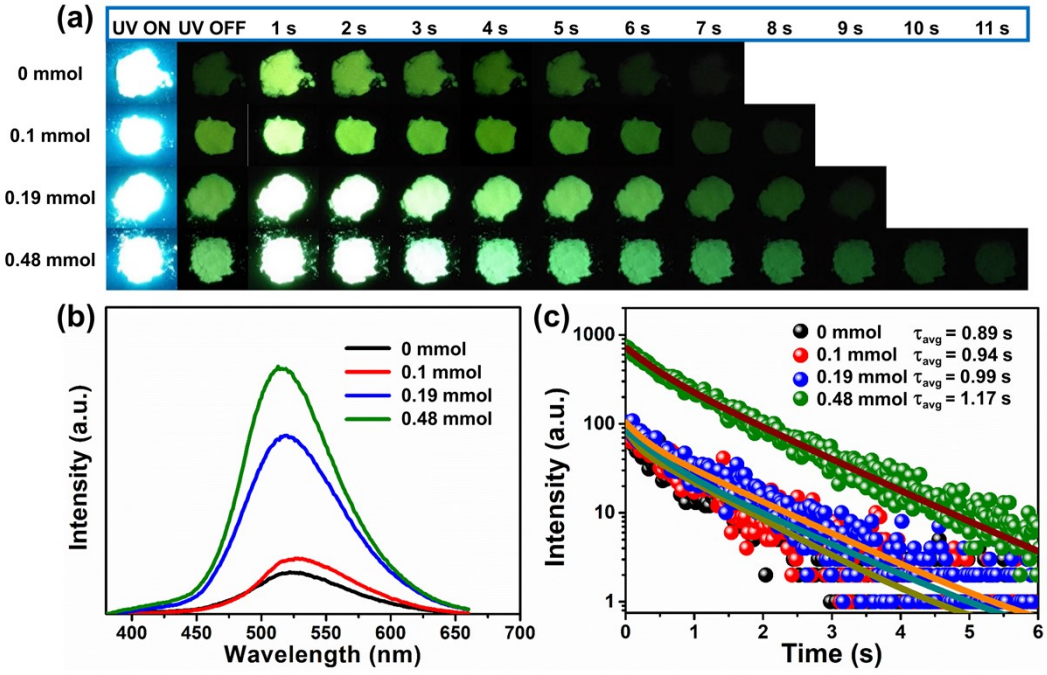

Fig. S11 (a) The photographs of F-BNDs(e) with different fluorine contents taken after the stoppage of 405 nm excitation. (b) The RTP spectra under 360 nm excitation and (c) time-resolved phosphorescence decay curves of F-BNDs(e) with different fluorine contents

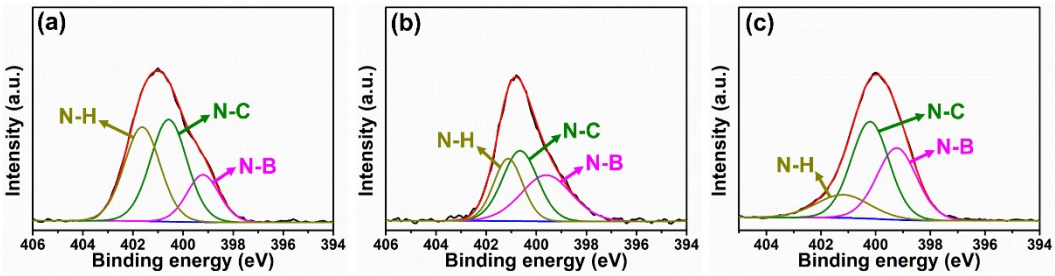

Fig. S12 High-resolution N1s spectra of (a) F-BNDs(e), (b) F-BNDs(p) and (c) F-BNDs(t).

High-resolution spectrum of N 1s bands demonstrates three peaks in 399.2, 400.6 and 401.6 eV, which are attributed to N-B, N-C/N-O and N-H bonds,[1, 2] respectively. The N-H bond implies the presence of $-NH_2$ groups.

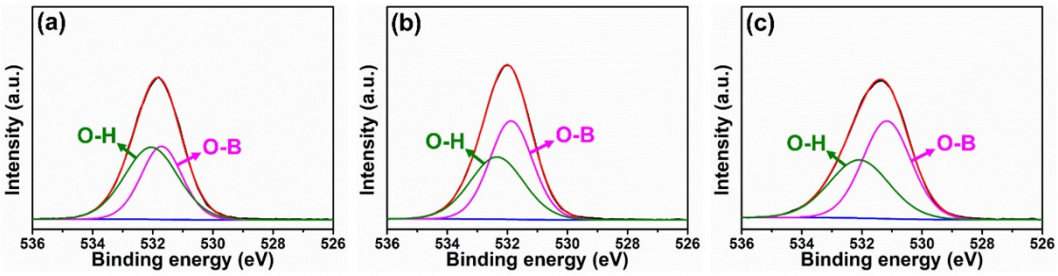

Fig. S13 High-resolution O1s spectra of (a) F-BNDs(e), (b) F-BNDs(p) and (c) F-BNDs(t).

The high-resolution O1s spectra exhibit two peaks, including O-B at 531.7 and O-H at 532.1 eV.[3]

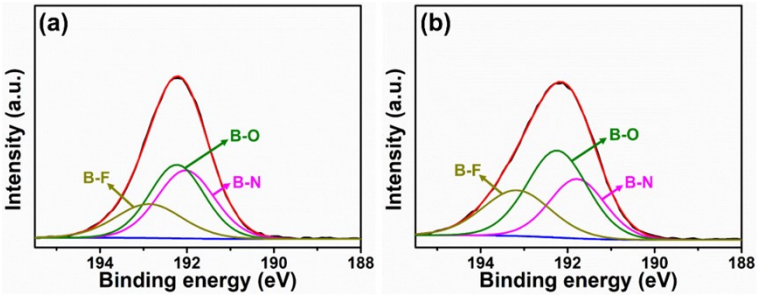

Fig. S14 High-resolution B1s spectra of (a) F-BNDs(p) and (b) F-BNDs(t).

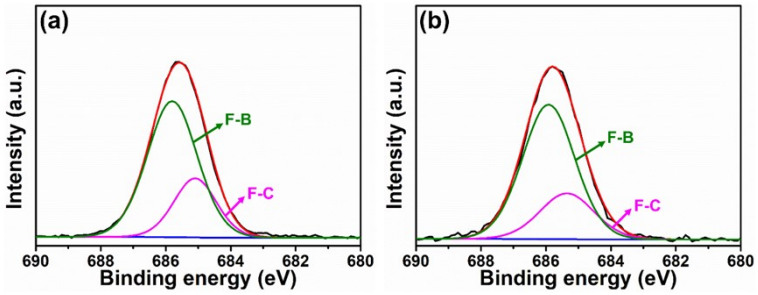

Fig. S15 High-resolution F1s spectra of (a) F-BNDs(p) and (b) F-BNDs(t).

The high-resolution spectrum of F1s shows two peaks at 684.9 and 685.6 eV for F-C and F-B bonds,[4, 5] respectively.

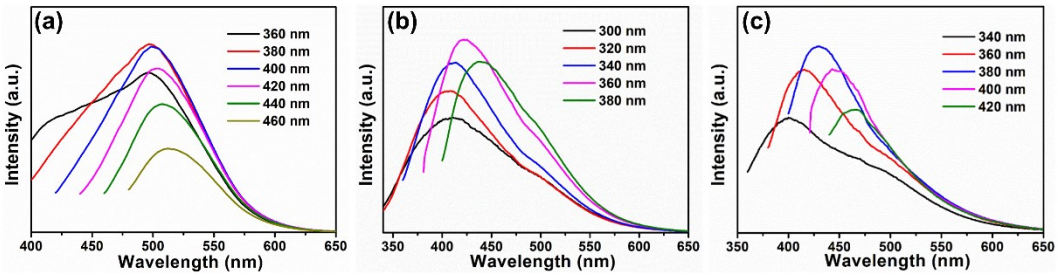

Fig. S16 FL emission spectra excited at different wavelengths of (a) F-BNDs(e), (b) F-BNDs(p) and (c) F-BNDs(t).

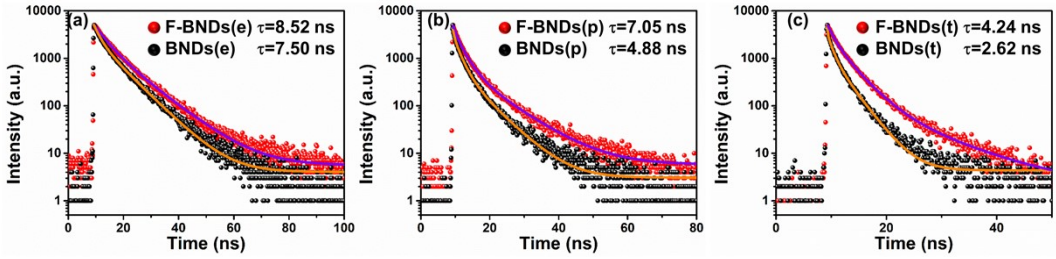

Fig. S17 (a) Time-resolved FL decay curves of F-BNDs(e) and BNDs(e) under 380 nm excitation. (b) Time-resolved FL decay curves of F-BNDs(p) and BNDs(p) under 380 nm excitation. (c) Time-resolved FL decay curves of F-BNDs(t) and BNDs(t) under 340 nm excitation.

The FL decay spectra of three F-BNDs are fitted to give FL lifetimes of 8.52, 7.05, and 4.24 ns for F-BNDs(e), F-BNDs(p) and F-BNDs(t), respectively. It is worth noting that the FL lifetimes of BNDs(e), BNDs(t) and BNDs(p) are 7.50, 4.88 and 2.62 ns, which are shorter than corresponding F-BNDs, respectively. These results should be attributed to the effect of hydrogen-bond network, suppressing the non-radiative transitions. Higher $-NH_2$ and -OH ratios are conducive to the formation of stronger inter- and intra-dot hydrogen-bond networks, exhibiting the longer FL and RTP lifetime.

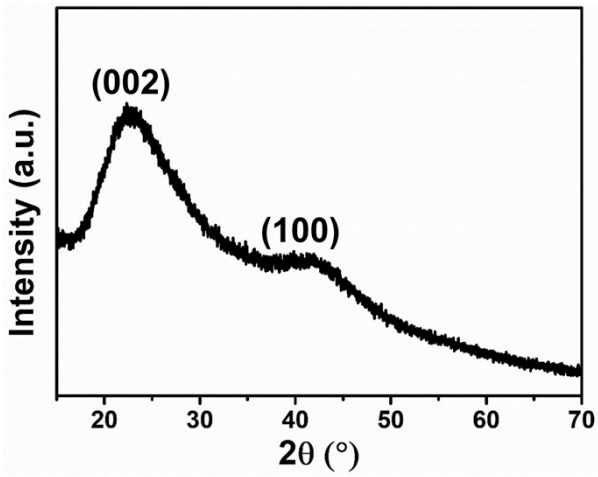

Fig. S18 The XRD pattern of the F-BNDs(e) after treatment at 700 ℃ for 0.5 h in air condition.

The F-BNDs(e) were treated at 700 ℃ for 0.5 h in air condition. After that, most of the sample was maintained and the phase composition is consistent with that before heating, exhibiting excellent thermal stability.

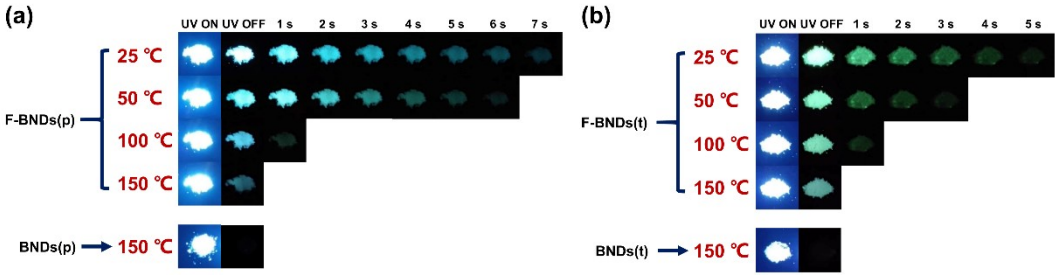

Fig. S19 The photographs of (a) F-BNDs(p) and (b) F-BNDs(t) taken after the stoppage of 405 nm excitation by varying temperatures from 25 to 150 °C and photographs of corresponding BNDs taken at 150 °C.

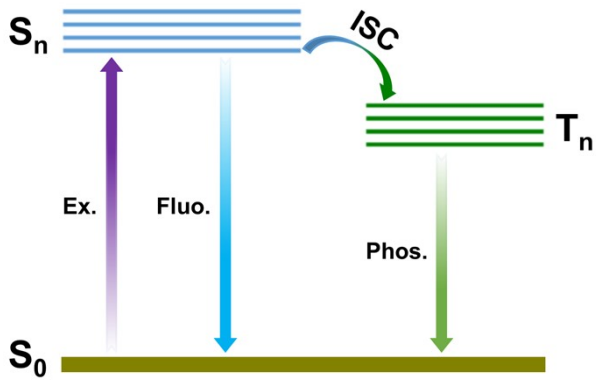

Fig. S20 Schematic illustration of the RTP emission mechanisms of the F-BNDs.

Tab. S1 Fitted parameters of the RTP decay curves of the F-BNDs and BNDs.

Sample	τ_1(s)	α_1(%)	τ_2(s)	α_2(%)	τ_{avg}(s)	Ø
F-BNDs(e)	0.393	15.48	1.222	84.52	1.175	1.210
F-BNDs(p)	0.211	23.69	1.131	73.61	1.074	1.176
F-BNDs(t)	0.055	42.51	0.415	57.49	0.383	1.557
BNDs(e)	0.051	1.67	0.896	98.33	0.895	1.134
BNDs(p)	0.148	29.25	0.553	70.75	0.513	1.169
BNDs(t)	0.021	63.50	0.129	36.50	0.106	1.325

Tab. S2 Phosphorescence lifetime comparison of some reported CD-based materials and F-BNDs.

Samples	Room-temperature Lifetime (ms)	High-temperature Lifetime (ms)	Ref.
B–CDs@PAM	637	—	6
M-CDs	243	—	7
FNCDs	1140	—	5
NCDs	1060	—	8
CDs/PVP	476	—	9
CNDs	193	—	10
MP-CDs	880	—	11
FP-CDs	175	—	12
CD@PVA	292	—	13
CNDs	1387	—	14
FCNDs	1210	—	15
F-BNDs(e)	**1175**	**250 (150 °C)**	**This work**

Tab. S3 The $-NH_2$ and -OH groups ratios of F-BNDs(e), F-BNDs(p) and F-BNDs(t) in N1s and O1s spectra.

Samples	$-NH_2$ (%)	-OH (%)
F-BNDs(e)	36.71	56.35
F-BNDs(p)	27.29	44.18
F-BNDs(t)	15.94	43.52

Supplementary video S1

The video S1 demonstrates that the F-BNDs(e) powder could emit green room temperature phosphorescence after the stoppage of 405 nm excitation, lasting over 10 s by the naked eyes.

References

1. M. Liu, Y. Xu, Y. Wang, X. Chen, X. Ji, F. Niu, Z. Song and J. Liu, *Adv. Opt. Mater.*, 2017, **5**, 1600661.
2. S. Angizi, F. Shayeganfar, M. H. Azar and A. Simchi, *Ceram. Int.*, 2020, **46**, 978-985.
3. S. Han, G. Lian, X. Zeng, Z. Cao, Q. Wang, D. Cui and C.-P. Wong, *Nano Res.*, 2020, **13**, 3261-3267.
4. A. Meiyazhagan, P. Serles, D. Salpekar, E. F. Oliveira, L. B. Alemany, R. Fu, G. Gao, T. Arif, R. Vajtai, V. Swaminathan, D. S. Galvao, V. N. Khabashesku, T. Filleter and P. M. Ajayan, *Adv. Mater.*, 2021, **33**, e2106084.
5. F. Liu, Z. Li, Y. Li, Y. Feng and W. Feng, *Carbon*, 2021, **181**, 9-15.
6. H. y. Wang, L. Zhou, H. m. Yu, X. d. Tang, C. Xing, G. Nie, H. Akafzade, S. y. Wang and W. Chen, *Adv. Opt. Mater.*, 2022, **10**, 2200678.
7. J. Bai, G. Yuan, X. Chen, L. Zhang, Y. Zhu, X. Wang and L. Ren, *Adv. Sci. (Weinh)*, 2022, **9**, e2104278.
8. Q. Li, M. Zhou, Q. Yang, Q. Wu, J. Shi, A. Gong and M. Yang, *Chem. Mater.*, 2016, **28**, 8221-8227.
9. Y. Liu, M. Al-Salihi, Y. Guo, R. Ziniuk, S. Cai, L. Wang, Y. Li, Z. Yang, D. Peng, K. Xi, Z. An, X. Jia, L. Liu, W. Yan and J. Qu, *Light Sci. Appl.*, 2022, **11**, 163.
10. S.-Y. Song, L.-Z. Sui, K.-K. Liu, Q. Cao, W.-B. Zhao, Y.-C. Liang, C.-F. Lv, J.-H. Zang, Y. Shang, Q. Lou, X.-G. Yang, L. Dong, K.-J. Yuan and C.-X. Shan, *Nano Res.*, 2021, **14**, 2231-2240.
11. K. Jiang, S. Hu, Y. Wang, Z. Li and H. Lin, *Small*, 2020, **16**, e2001909.
12. B. Zhao, R. Yu, K. Xu, C. Zou, H. Ma, S. Qu and Z. a. Tan, *J. Mater. Chem. C*, 2021, **9**, 15577-15582.
13. X. Bao, E. V. Ushakova, E. Liu, Z. Zhou, D. Li, D. Zhou, S. Qu and A. L. Rogach, *Nanoscale*, 2019, **11**, 14250-14255.